Quantum-enhanced weak absorption estimation with correlated photons

Zhucheng Zhang,[1] Xue Zhang,[1] Jing Liu,[2] and Hui Dong[1, *]

[1]*Graduate School of China Academy of Engineering Physics, Beijing 100193, China*

[2]*National Precise Gravity Measurement Facility, MOE Key Laboratory of Fundamental Physical Quantities Measurement, School of Physics, Huazhong University of Science and Technology, Wuhan 430074, China*

(Dated: August 27, 2024)

Absorption estimation, the base of spectroscopy, is crucial for probing the composition and dynamics of matter. Conventional methods of estimation rely on coherent laser sources, and in turn suffer from inherent limitations in estimating weak absorption. Here we propose a new measurement strategy with correlated photons to determine the weak absorption by distinguishing the output with and without photons, dubbed as the on-off measurement. Our implementation within the strategy allows the estimation precision to reach the ultimate quantum limit. We demonstrate that absorption spectroscopy that incorporates quantum correlations is capable of estimating weak absorption down to a single-photon level, even in noisy environments, achieving a precision comparable to that obtained through several hundred photons in conventional absorption spectroscopy. By introducing the quantum correlations, our work avoids the occurrence of light-induced damage while breaking the classical inherent limitations in spectroscopy.

INTRODUCTION

Laser spectroscopy, rooted in the subtle interaction between light and matter, is commonly employed for the purpose of identifying complex mixtures of chemical compounds and unraveling the intricacies of chemical reactions with an unprecedented temporal resolution, diving into the femtosecond realm [1–5]. The effectiveness of spectroscopic detection hinges considerably on the distinctive classical attributes of lasers [6–9], such as their intensity, coherence, and duration. Conventional spectroscopy faces inherent limitations due to the shot noise, determined by the statistical properties of photons [10]. Increasing light intensity has been a viable strategy to mitigate shot-noise effects. However, this strategy inevitably causes light-induced damage to fragile samples [11, 12]. Utilizing the non-classical properties of lasers [13–17], such as quantum photon correlations, seems to be the only way to break through these limitations.

It has been well-established that quantum correlations allow more information to be extracted per photon in optical measurements [18]. Such quantum correlations are used routinely to improve the sensitivity and resolution of phase measurement in the realm of physics, such as Mach-Zehnder interferometers [19–21], and laser interferometric gravitational wave detectors [22]. Currently, ongoing efforts are devoted to exploring the potential of quantum correlations in breaking the classical constraints in laser spectroscopy for investigating the absorption and emission of natural photosynthetic complexes [23], increasing the spatial resolution of microscopy [15, 24–28], and improving the measurement precision of material absorption [17, 29–41]. By exploiting quantum correlations, it is promising to design novel spectroscopic techniques that can surpass the classical limitations.

In this work, we design a new measurement strategy for absorption estimation that leverages quantum correlations between photons. Absorption spectroscopy is a well-used technique to characterize chemical and biological samples by measuring their absorption of electromagnetic radiation [42, 43]. Each substance has a distinct absorption spectrum that can be utilized for fingerprint recognition of materials. However, conventional absorption estimation methods, predominantly relying on coherent laser sources, encounter inherent limitations when it comes to determining weak absorption, especially in noisy environments [13, 14]. We show that the absorption spectroscopy with quantum correlations allows us to break through the classical limitations and to measure the weak absorption effectively down to a single-photon level within the noisy environment.

RESULTS

Quantum absorption spectroscopy. During its interaction with the sample, the incident light, denoted by the creation operator $a^\dagger$, is attenuated and combined with environmental thermal noise [44], namely,

$$a^\dagger \rightarrow \sqrt{1-\alpha}a^\dagger + \sqrt{\alpha}e^\dagger, \qquad (1)$$

where $\alpha \in [0,1]$ is the absorption coefficient of the sample and e is the environmental mode with average photon number n_{th} to characterize the intensity of the thermal noise. Then the information about the sample, i.e., absorption coefficient, is encoded into the transmitted light. As shown in Fig. 1a, our quantum absorption spectroscopy (QAS) employs a quantum source of correlated signal-idler lights prepared by spontaneous parametric down conversion (SPDC) in a nonlinear media. The signal light illuminates the sample, while the idler light serves as an ancilla and does not directly participate in the interaction with the sample. The two beams
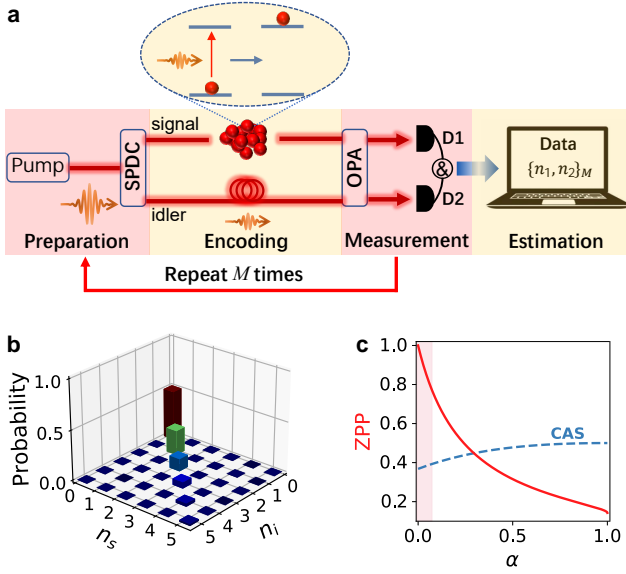
FIG. 1. **Experimental model for quantum absorption spectroscopy**. **a**, Correlated signal-idler lights, prepared by spontaneous parametric down conversion (SPDC) in a nonlinear media, are used to estimate the absorption of the sample, in which the signal light interacts with the sample and the idler light acts as an ancilla. At the measurement end, the transmitted light and the idler light undergo an optical parametric amplification process through the utilization of an optical parametric amplifier (OPA). Additionally, two detectors, D1 and D2, are employed for joint photon counting. The above measurement process is then repeated independently M times. Finally, these repeated measurement data $\{n_1, n_2\}_M$ are statistically analyzed to estimate the absorption of the sample. **b**, Probability of the incident signal-idler lights having n_s photons and n_i photons respectively, where the average photon number of each mode is one. **c**, Zero-photon probability (ZPP) $P(\{0,0\}|\alpha)$ obtained at the measurement end is plotted as a function of the absorption coefficient α, where the counterpart in the conventional absorption spectroscopy (CAS) is illustrated for comparison. The related parameters used in the numerical simulation are: $n_a = 1$, and $n_{\text{th}} = 1$.

of light are in a two-mode squeezed vacuum state (see the Methods section), which possess identical photon number distribution, as illustrated in Fig. 1b. By determining the photon number of the idler light, quantum correlations between them allow one to indirectly infer the photon number of the signal light illuminating the sample. At the measurement end, an optical parametric amplifier (OPA) is applied to perform a two-mode squeezing operation on the transmitted and the idler light. Two detectors (D1 and D2) are employed for joint photon counting, yielding outcomes n_1 and n_2 with the theoretical probability $P(\{n_1, n_2\}|\alpha)$ in the output signal and idler lights, respectively (details in Supplementary Material section 1 [45]). This measurement process is independently repeated multiple times. The data $\{n_1, n_2\}_M$ obtained from M repeated measurements are processed and analyzed utilizing the statistical inference method

to extract the absorption coefficient α. The estimated value $\hat{\alpha}$ with the M times of measurements is obtained as $\hat{\alpha} = \int \alpha P(\alpha|\{n_1, n_2\}_M)\mathrm{d}\alpha$, in which $P(\alpha|\{n_1, n_2\}_M)$ is a probability deduced from the M repeated measurement data $\{n_1, n_2\}_M$ through the Bayes' rule (see the Methods section). Additionally, the estimated variance $\delta^2\hat{\alpha}$ is determined via the following equation,

$$\delta^2\hat{\alpha} = \int \alpha^2 P(\alpha|\{n_1, n_2\}_M)\mathrm{d}\alpha - \left(\int \alpha P(\alpha|\{n_1, n_2\}_M)\mathrm{d}\alpha\right)^2. \quad (2)$$

The conventional absorption spectroscopy (CAS) typically employs an input of a laser under the coherent state [42, 43]. And the average number $\langle a^\dagger a\rangle_{\text{out}}$ of output photons is measured without photon number counting, namely, intensity measurement. The estimation is performed by comparing a known average number $\langle a^\dagger a\rangle_{\text{in}}$ of input photons and the measured average number of output photons, i.e., $\hat{\alpha} = 1 - \langle a^\dagger a\rangle_{\text{out}}/\langle a^\dagger a\rangle_{\text{in}}$, with the estimated variance as $\delta^2\hat{\alpha} = \Delta^2(a^\dagger a)/|\partial\langle a^\dagger a\rangle_{\text{out}}/\partial\alpha|^2$ (details in Supplementary Material section 2 [45]), in which $\Delta^2(a^\dagger a) = \langle(a^\dagger a)^2\rangle_{\text{out}} - \langle a^\dagger a\rangle_{\text{out}}^2$ is the variance of output photons. Figure 2a and 2b show the estimated variances for CAS as functions of the absorption coefficient α and the average number n_a of input photons, respectively. The dashed lines show the so-called shot-noise limit in CAS. Given a constant input light intensity, one can see that the CAS exhibits high estimation variance in the region of weak absorption, especially in noisy environments, as shown in Fig. 2a. Meanwhile, in a noisy environment, the estimated variance tends towards the shot-noise limit as the number of input photons increases significantly [13], as illustrated in Fig. 2b. Clearly, CAS exhibits limitations in measuring weak absorption samples in noisy environments.
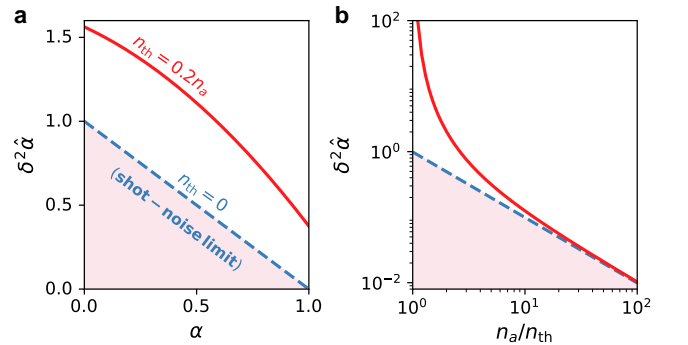

FIG. 2. **Estimated variance $\delta^2\hat{\alpha}$ in conventional absorption spectroscopy**. Estimated variance as a function of (**a**) the absorption coefficient α and (**b**) the average number n_a of input photons. The shot-noise limit is the measurement precision limit in CAS, i.e., $\delta^2\hat{\alpha} = (1 - \alpha)/n_a$, which can only be achieved when all noise is eliminated. The related parameters used in the numerical simulation are: **a**, $n_a = 1$, $n_{\text{th}} = 0, 0.2n_a$, and **b**, $n_{\text{th}} = 1$, $\alpha = 0.01$.
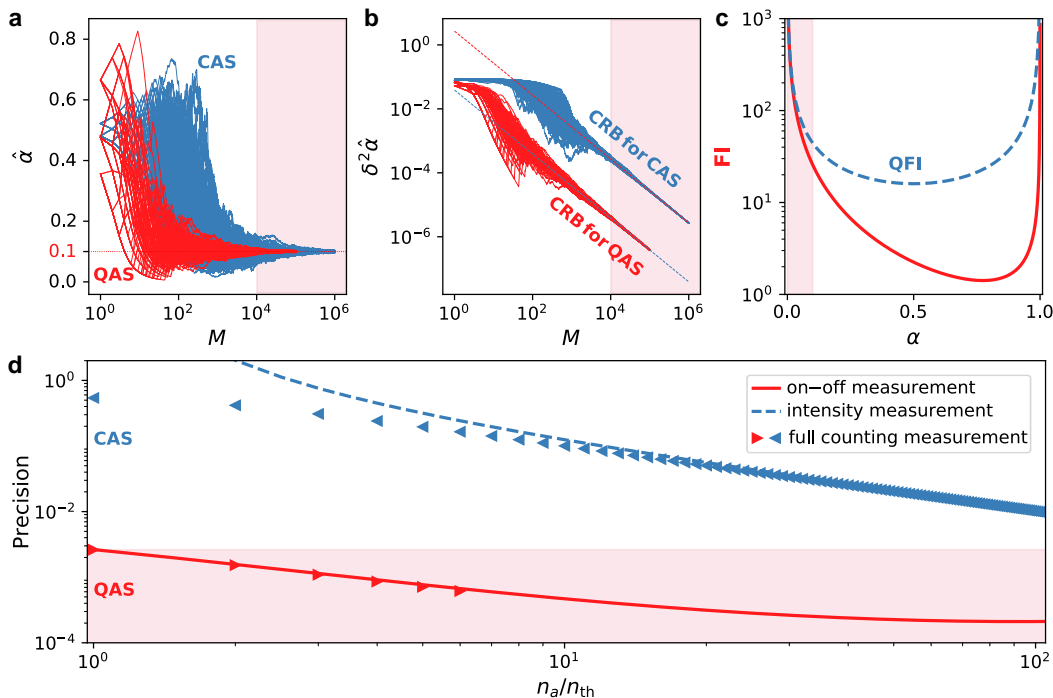
FIG. 3. **Quantum-enhanced weak absorption estimation**. **a**, **b**, Estimated value $\hat{\alpha}$ and estimated variance $\delta^2\hat{\alpha}$, associated with the on-off measurement, are plotted as a function of the number M of repeated measurements in 100 rounds of simulation experiments, where the measurement data $\{n_1, n_2\}_M$ in each round of experiments are generated by the Monte Carlo simulation and the true value of the absorption coefficient is set as 0.1. **c**, Fisher information (FI), associated with the on-off measurement, is plotted as a function of the absorption coefficient α, where the quantum Fisher information (QFI) is plotted as a comparison. **d**, Estimation precision is plotted as a function of the average number of photons n_a in the incident signal light, where the on-off measurement and the full counting measurement are considered. To highlight quantum-enhanced estimation precision, the intensity measurement and full counting measurement in CAS are plotted. The related parameters used here are: **a**, **b**, **c**, $n_a = 1$ and $n_{\text{th}} = 1$; **d**, $n_{\text{th}} = 1$ and $\alpha = 0.01$. The estimation precision based on the full counting measurement is finished with an open-source toolkit for quantum parameter estimation [46].

Quantum-enhanced sensitivity for weak absorption. In contrast to CAS, the utilization of quantum-correlated light sources offers inherent benefits for estimating weak absorption samples. The signal-idler lights generated through the SPDC process in our QAS have a non-classical photon number distribution (see Fig. 1b), exhibiting quantum correlations. Quantum-correlated light sources have been widely used in optical measurement [19–22] and imaging [15, 24–28], demonstrating significant improvement in sensitivity and resolution. Used here they allow the enhancement of sensitivity to weak absorption samples, even in environments where the input signal is disturbed by the thermal noise.

To illustrate physical origin of quantum enhancement, we investigate, in Fig. 1c, the change of the probability $P(\{0,0\}|\alpha)$ of detecting zero photons at the measurement end with the absorption coefficient α. During the measurement process, we utilize OPA to perform a two-mode squeezing operation, which anti-squeezes the output signal-idler lights (see the Methods section). In the extreme case of full transmission, such anti-squeeze results in zero-photon probability (ZPP) for both detectors, namely, $P(\{0,0\}|\alpha=0) = 1$. And the ZPP remains dom-

inant, ensured by the quantum correlations, in the weak absorption region of the sample. Such properties allow a simple measurement scheme discussed later. The sensitivity of the QAS is mainly determined by the change rate of $P(\{0,0\}|\alpha)$ upon a small change of α, namely $|\mathrm{d}P(\{0,0\}|\alpha)/\mathrm{d}\alpha|$, which is large in the weak absorption region. Such a picture illustrates that quantum correlations will enable more information to be gained in the weak absorption region of the sample, thereby improving the sensitivity of absorption estimation. The exact explanation for quantum enhancement is presented in section 3 of Supplementary Material [45].

Quantum-enhanced absorption estimation. To demonstrate quantum-enhanced absorption estimation, we investigate the variation of estimated value $\hat{\alpha}$ under multiple repeated measurements. Noticing the fact that the ZPP $P(\{0,0\}|\alpha)$ dominates in the weak absorption region of the sample, we simplify the measurement scheme for the two detectors. The two detectors only need to distinguish whether there is photon counting, dubbed as the on-off measurement, yielding four types of measurement outcomes, namely, $\{0,0\}$, $\{0,\emptyset\}$, $\{\emptyset,0\}$, and $\{\emptyset,\emptyset\}$, with theoretical probabilities $P(\{0,0\}|\alpha)$,

$P(\{0, \emptyset\}|\alpha)$, $P(\{\emptyset, 0\}|\alpha)$, and $P(\{\emptyset, \emptyset\}|\alpha)$, respectively, in which the symbol $\emptyset$ represents that the detector has photon counts (see the Methods section). This type of on-off detector has been extensively utilized in optical phase estimation [47–49], significantly reducing the requirement for high-performance detectors in practical experiments. As shown in Fig. 3a, we demonstrate the variation of the estimated value $\hat{\alpha}$ with respect to the number M of repeated measurements in 100 rounds of simulation experiments, in which the measurement data $\{n_1, n_2\}_M$ in each round of experiments are generated through Monte Carlo simulation (details in Methods section). The curves in the figure illustrate that with the input of correlated signal-idler lights, the estimated value converges asymptotically to the true value, namely, 0.1, in each round of simulation experiments. Compared with CAS, the introduction of quantum correlations significantly reduces the number for repeated measurements in each round of experiments when converging to the true value.

Figure 3b demonstrates the variation of the estimated variance $\delta^2\hat{\alpha}$ with the number M of repeated measurements. The results show that under the same repeat times as CAS, quantum correlations guarantee a superior estimation accuracy in determining the absorption of the sample. Additionally, the curves further reveal that the estimated variance gradually diminishes in each round of experiments, ultimately converging towards a specific bound, as the number of measurements increases. This bound is the well-known Cramér-Rao bound (CRB) in parameter estimation theory [50–58], namely, $1/(MF)$, in which F is the Fisher information (FI), associated with an actual measurement scheme, to characterize the information extracted.

Reaching the ultimate precision limit. The performance of the current on-off measurement scheme is evaluated in Fig. 3c with FI as a function of α, see the solid curve. The large FI at the small absorption side demonstrates that quantum correlations enhance sensitivity for the weak absorption samples in noisy environments. An ultimate upper bound for FI exists and is termed quantum Fisher information (QFI) $\mathcal{F}$, with the explicit form for our QAS as (see Supplementary Material section 4 [45])

$$\mathcal{F} = \frac{n_a + n_{\text{th}} + 2n_a n_{\text{th}}}{\alpha(1 - \alpha)}. \tag{3}$$

In the weak absorption region, the FI in our QAS is only different from the ultimate upper bound with a small deviation. It is clear that our on-off measurement scheme achieves the ultimate precision limit in estimating the weak absorption in noisy environments.

The on-off measurement scheme is capable of estimating weak absorption coefficient with a limited number of photons. In Fig. 3d, the estimation precision, $\delta^2\hat{\alpha}$, is plotted as a function of the average number of photons n_a of the incident signal light for both QAS (solid curve) and CAS (dashed curve). The results show clear advantages

of QAS over CAS in estimating the weak absorption. We demonstrate that our on-off measurement scheme allows the estimation of the weak absorption down to a single-photon level within the noisy environment. And an average one-photon correlation source can achieve the estimation precision comparable to that achieved with several hundred photons in CAS. The low photon number in the current on-off measurement scheme allows us to avoid the light-induced damage to the sample, compared with the common strategy of increasing light intensity to mitigate the shot noise in CAS [42, 43], while achieving comparable estimation precision.

One potential improvement for precision is to utilize the full counting measurement [59–61], where the exact photon number is detected to reveal the full distribution $P(\{n_1, n_2\}|\alpha)$, allowing for maximum information extraction. In Fig. 3d, we further show the estimation precision obtained with the full counting measurement. We demonstrate that our QAS (right triangle) offers more information on the sample, enabling a superior level of estimation precision over CAS (left triangle). Importantly, the precision in our QAS achieved through the on-off measurement is also better than that in CAS with the full counting measurement.

DISCUSSION

By reporting absorption spectroscopy with quantum-enhanced sensitivity and using it to improve estimation precision for samples with weak absorption in noisy environments, our study quantitatively demonstrates the long-recognized potential of quantum correlations to overcome classical limitations in spectroscopy. Our implementation within the on-off measurement scheme provides the capacity to reach the ultimate precision limit in noisy environments in weak absorption regions. We show that absorption spectroscopy that incorporates quantum correlations can measure the weak absorption down to the single-photon level in noisy environments, with precision comparable to that achieved by several hundred photons in CAS. This quantum absorption spectroscopy represents a pivotal application to overcome the classical constraints on sensitivity and precision of existing high-performance laser spectroscopy.

Building upon considerations of thermal noise in the sample environment, we analyze in detail the impacts of factors such as the loss of the input light source, the dark counts of the detector, and the anti-squeeze operation of the OPA on the precision improvement brought by quantum correlations, see section 5 of our supplementary material [45]. We demonstrate that the on-off measurement scheme remains effective in our QAS despite the influence of these factors, allowing us to break through the shot-noise limit of CAS.

METHODS

Initial quantum state. The signal-idler lights, generated through the SPDC process, are in a two-mode squeezed vacuum state [62],

$$|\psi\rangle_{\text{tmsv}} = S(\xi)|0,0\rangle, \quad (4)$$

where $S(\xi) = \exp(\xi^* ab - \xi a^\dagger b^\dagger)$ is the two-mode squeezed operator, $\xi = |\xi|e^{i\theta}$ is the squeezed parameter, $a(a^\dagger)$ and $b(b^\dagger)$ are the annihilation (creation) operators of the signal and idler lights, respectively. The two-mode squeezed vacuum state is a two-mode entangled state, which can be represented as $|\psi\rangle_{\text{tmsv}} = \sum_{n_s,n_i} C_{n_s,n_i}|n_s,n_i\rangle$ in the number-state space, in which $C_{n_s,n_i} = (-e^{i\theta}\tanh|\xi|)^n/\cosh|\xi|$ if $n_s = n_i = n$, and $C_{n_s,n_i} = 0$ if $n_s \neq n_i$, as illustrated in Fig. 1b.

Two-mode squeezing operation generated by OPA. The OPA, based on a nonlinear optical crystal, performs a two-mode squeezed operation on the transmitted light and the idler light [62]. For the case of full transmission, i.e., the absorption coefficient $\alpha = 0$, the quantum state at the measurement end is

$$|\psi\rangle = S(\zeta)|\psi\rangle_{\text{tmsv}}, \quad (5)$$

where $S(\zeta)$ is the two-mode squeezed operator of OPA, and $\zeta = |\zeta|e^{i\Theta}$ is the squeezed parameter. When $\zeta = -\xi$, such a two-mode squeezing operation anti-squeezes the output signal-idler lights, resulting in zero-photon probability for both detectors at the measurement end, as illustrated in Fig. 1c.

Monte Carlo simulation for the measurement data. With on-off detectors, the repeated measurement data $\{n_1, n_2\}_M$ includes four types, i.e., $\{0,0\}$, $\{0,\emptyset\}$, $\{\emptyset,0\}$, and $\{\emptyset,\emptyset\}$, with theoretical probabilities,

$$P(\{0,0\}|\alpha) = P(\{n_1=0, n_2=0\}|\alpha), \quad (6)$$

$$P(\{0,\emptyset\}|\alpha) = \sum_{n_2=1}^\infty P(\{0,n_2\}|\alpha), \quad (7)$$

$$P(\{\emptyset,0\}|\alpha) = \sum_{n_1=1}^\infty P(\{n_1,0\}|\alpha), \quad (8)$$

$$P(\{\emptyset,\emptyset\}|\alpha) = 1 - P(\{0,0\}|\alpha) - P(\{0,\emptyset\}|\alpha) - P(\{\emptyset,0\}|\alpha), \quad (9)$$

respectively. The specific expressions of the above probabilities are given in Supplementary Material section 1 [45]. And the measurement data $\{n_1, n_2\}_M$ are generated through Monte Carlo simulation [63–65], as follows,

1. Choose any one of the four types as the first observation $\{n_1, n_2\}_M^{(1)}$.
2. Propose a candidate $\{n_1, n_2\}$ for the next observation by picking from the four types.
3. Calculate the acceptance ratio, $\Upsilon = P(\{n_1,n_2\}|\alpha)/P(\{n_1,n_2\}_M^{(1)}|\alpha)$, which is used to determine whether the candidate $\{n_1, n_2\}$ becomes the next observation.
4. Generate a uniform random number $u \in [0,1]$. If $u \leq \Upsilon$, accept the candidate by setting $\{n_1,n_2\}_M^{(2)} = \{n_1,n_2\}$. If $u > \Upsilon$, reject the candidate and set $\{n_1,n_2\}_M^{(2)} = \{n_1,n_2\}_M^{(1)}$.
5. Repeat steps 2 to 4. Here, the number of repetitions is 10^5.

We then perform statistical inference on these measurement data. Using the first observation $\{n_1,n_2\}_M^{(1)}$, we have the posterior probability distribution,

$$P\left(\alpha|\{n_1,n_2\}_M^{(1)}\right) = \frac{P\left(\{n_1,n_2\}_M^{(1)}|\alpha\right)P(\alpha)}{\int P\left(\{n_1,n_2\}_M^{(1)}|\alpha\right)P(\alpha)d\alpha}, \quad (10)$$

through the Bayes' rule, in which $P(\alpha)$ is the current prior probability distribution that is assumed to be uniform in the regime $[0,1]$. The prior distribution is then updated with $P(\alpha|\{n_1,n_2\}_M^{(1)})$. After iterating M times, we can obtain the probability $P(\alpha|\{n_1,n_2\}_M)$ conditional on the M repeated measurement data $\{n_1,n_2\}_M$.

DATA AVAILABILITY

The data that support the findings of this study are available from H.D. upon reasonable request.

CODE AVAILABILITY

The code used in this study is available from H.D. upon reasonable request.

[1] A. L. Schawlow, Spectroscopy in a new light, Rev. Mod. Phys. **54**, 697 (1982).
[2] W. Demtröder, *Laser spectroscopy*, Vol. 2 (Springer, 1982).
[3] R. W. Solarz and J. A. Paisner, *Laser spectroscopy and its applications* (Routledge, 2017).
[4] S. Stenholm, *Foundations of laser spectroscopy* (Courier Corporation, 2012).
[5] P. Hannaford, *Femtosecond laser spectroscopy* (Springer Science & Business Media, 2004).
[6] A. Yariv and J. Gordon, The laser, Proc. IEEE **51**, 4 (1963).
[7] W. T. Silfvast, *Laser fundamentals* (Cambridge university press, 2004).
[8] J. Hecht, Short history of laser development, Opt. Eng. **49**, 091002 (2010).

[9] K. Shimoda, *Introduction to laser physics*, Vol. 44 (Springer, 2013).

[10] M. A. Taylor and W. P. Bowen, Quantum metrology and its application in biology, Phys. Rep. **615**, 1 (2016).

[11] A. Hopt and E. Neher, Highly nonlinear photodamage in two-photon fluorescence microscopy, Biophys. J. **80**, 2029 (2001).

[12] Y. Fu, H. Wang, R. Shi, and J.-X. Cheng, Characterization of photodamage in coherent anti-stokes raman scattering microscopy, Opt. Express **14**, 3942 (2006).

[13] A. Monras and M. G. A. Paris, Optimal quantum estimation of loss in bosonic channels, Phys. Rev. Lett. **98**, 160401 (2007).

[14] G. Adesso, F. Dell'Anno, S. De Siena, F. Illuminati, and L. A. M. Souza, Optimal estimation of losses at the ultimate quantum limit with non-gaussian states, Phys. Rev. A **79**, 040305(R) (2009).

[15] C. A. Casacio, L. S. Madsen, A. Terrasson, M. Waleed, K. Barnscheidt, B. Hage, M. A. Taylor, and W. P. Bowen, Quantum-enhanced nonlinear microscopy, Nature **594**, 201 (2021).

[16] A. Belsley, Quantum-enhanced absorption spectroscopy with bright squeezed frequency combs, Phys. Rev. Lett. **130**, 133602 (2023).

[17] H. Shi, Z. Zhang, S. Pirandola, and Q. Zhuang, Entanglement-assisted absorption spectroscopy, Phys. Rev. Lett. **125**, 180502 (2020).

[18] R. Slusher, Quantum optics in the'80s, Opt. Photon. News **1**, 27 (1990).

[19] P. M. Anisimov, G. M. Raterman, A. Chiruvelli, W. N. Plick, S. D. Huver, H. Lee, and J. P. Dowling, Quantum metrology with two-mode squeezed vacuum: Parity detection beats the heisenberg limit, Phys. Rev. Lett. **104**, 103602 (2010).

[20] P. Yin, X. Zhao, Y. Yang, Y. Guo, W.-H. Zhang, G.-C. Li, Y.-J. Han, B.-H. Liu, J.-S. Xu, G. Chiribella, *et al.*, Experimental super-heisenberg quantum metrology with indefinite gate order, Nat. Phys. **19**, 1122 (2023).

[21] Y.-F. Guo, W. Zhong, L. Zhou, and Y.-B. Sheng, Supersensitivity of kerr phase estimation with two-mode squeezed vacuum states, Phys. Rev. A **105**, 032609 (2022).

[22] J. Aasi, J. Abadie, B. Abbott, R. Abbott, T. Abbott, M. Abernathy, C. Adams, T. Adams, P. Addesso, R. Adhikari, *et al.*, Enhanced sensitivity of the ligo gravitational wave detector by using squeezed states of light, Nat. Photon. **7**, 613 (2013).

[23] Q. Li, K. Orcutt, R. L. Cook, J. Sabines-Chesterking, A. L. Tong, G. S. Schlau-Cohen, X. Zhang, G. R. Fleming, and K. B. Whaley, Single-photon absorption and emission from a natural photosynthetic complex, Nature **619**, 300 (2023).

[24] T. Ono, R. Okamoto, and S. Takeuchi, An entanglement-enhanced microscope, Nat. Commun. **4**, 2426 (2013).

[25] P.-A. Moreau, E. Toninelli, T. Gregory, and M. J. Padgett, Imaging with quantum states of light, Nat. Rev. Phys. **1**, 367 (2019).

[26] N. Samantaray, I. Ruo-Berchera, A. Meda, and M. Genovese, Realization of the first sub-shot-noise wide field microscope, Light Sci. Appl. **6**, e17005 (2017).

[27] M. Li, C.-L. Zou, D. Liu, G.-P. Guo, G.-C. Guo, and X.-F. Ren, Enhanced absorption microscopy with correlated photon pairs, Phys. Rev. A **98**, 012121 (2018).

[28] J. Sabines-Chesterking, A. McMillan, P. Moreau, S. Joshi, S. Knauer, E. Johnston, J. Rarity, and J. Matthews, Twin-beam sub-shot-noise raster-scanning microscope, Opt. Express **27**, 30810 (2019).

[29] E. Jakeman and J. Rarity, The use of pair production processes to reduce quantum noise in transmission measurements, Opt. Commun. **59**, 219 (1986).

[30] P. S. Ribeiro, C. Schwob, A. Maître, and C. Fabre, Sub-shot-noise high-sensitivity spectroscopy with optical parametric oscillator twin beams, Opt. Lett. **22**, 1893 (1997).

[31] M. M. Hayat, A. Joobeur, and B. E. Saleh, Reduction of quantum noise in transmittance estimation using photon-correlated beams, JOSA A **16**, 348 (1999).

[32] G. Brida, M. Genovese, and I. Ruo Berchera, Experimental realization of sub-shot-noise quantum imaging, Nat. Photonics **4**, 227 (2010).

[33] D. A. Kalashnikov, A. V. Paterova, S. P. Kulik, and L. A. Krivitsky, Infrared spectroscopy with visible light, Nat. Photonics **10**, 98 (2016).

[34] G. Scarcelli, A. Valencia, S. Gompers, and Y. Shih, Remote spectral measurement using entangled photons, Appl. Phys. Lett. **83**, 5560 (2003).

[35] A. Yabushita and T. Kobayashi, Spectroscopy by frequency-entangled photon pairs, Phys. Rev. A **69**, 013806 (2004).

[36] P.-A. Moreau, J. Sabines-Chesterking, R. Whittaker, S. K. Joshi, P. M. Birchall, A. McMillan, J. G. Rarity, and J. C. Matthews, Demonstrating an absolute quantum advantage in direct absorption measurement, Sci. Rep. **7**, 6256 (2017).

[37] R. Whittaker, C. Erven, A. Neville, M. Berry, J. O'Brien, H. Cable, and J. Matthews, Absorption spectroscopy at the ultimate quantum limit from single-photon states, New J. Phys. **19**, 023013 (2017).

[38] E. Losero, I. Ruo-Berchera, A. Meda, A. Avella, and M. Genovese, Unbiased estimation of an optical loss at the ultimate quantum limit with twin-beams, Sci. Rep. **8**, 7431 (2018).

[39] J. Wang, R. L. d. M. Filho, G. S. Agarwal, and L. Davidovich, Quantum advantage of time-reversed ancilla-based metrology of absorption parameters, Phys. Rev. Res. **6**, 013034 (2024).

[40] R. Jonsson and R. Di Candia, Gaussian quantum estimation of the loss parameter in a thermal environment, J. Phys. A: Math. Theor. **55**, 385301 (2022).

[41] F. Li, T. Li, M. O. Scully, and G. S. Agarwal, Quantum advantage with seeded squeezed light for absorption measurement, Phys. Rev. Appl. **15**, 044030 (2021).

[42] W. L. Butler, Absorption spectroscopy in vivo theory and application, Annu. Rev. Plant Physiol. **15**, 451 (1964).

[43] U. Platt, J. Stutz, U. Platt, and J. Stutz, *Differential absorption spectroscopy* (Springer, 2008).

[44] C. Weedbrook, S. Pirandola, R. García-Patrón, N. J. Cerf, T. C. Ralph, J. H. Shapiro, and S. Lloyd, Gaussian quantum information, Rev. Mod. Phys. **84**, 621 (2012).

[45] See supplemental material for additional details of derivation and calculation.

[46] M. Zhang, H.-M. Yu, H. Yuan, X. Wang, R. Demkowicz-Dobrzański, and J. Liu, Quanestimation: An open-source toolkit for quantum parameter estimation, Phys. Rev. Res. **4**, 043057 (2022).

[47] T. Lipfert, J. Sperling, and W. Vogel, Homodyne detection with on-off detector systems, Phys. Rev. A **92**,

053835 (2015).

[48] D. Gatto, P. Facchi, F. A. Narducci, and V. Tamma, Distributed quantum metrology with a single squeezed-vacuum source, Phys. Rev. Res. **1**, 032024 (2019).

[49] D. Gatto, P. Facchi, and V. Tamma, Heisenberg-limited estimation robust to photon losses in a mach-zehnder network with squeezed light, Phys. Rev. A **105**, 012607 (2022).

[50] H. Cramér, *Mathematical methods of statistics* (Princeton university press, 1999).

[51] R. A. Fisher, On the dominance ratio, Proc. R. Soc. Edinburgh **42**, 321 (1923).

[52] C. W. Helstrom, *Quantum detection and estimation theory* (Academic Press, 1976).

[53] A. S. Holevo, *Probabilistic and statistical aspects of quantum theory* (North-Holland Publishing Company, 1982).

[54] S. L. Braunstein and C. M. Caves, Statistical distance and the geometry of quantum states, Phys. Rev. Lett. **72**, 3439 (1994).

[55] M. G. Paris, Quantum estimation for quantum technology, Int. J. Quant. Inf **7**, 125 (2009).

[56] H. M. Wiseman and G. J. Milburn, *Quantum measurement and control* (Cambridge university press, 2009).

[57] J. Liu, H. Yuan, X.-M. Lu, and X. Wang, Quantum fisher information matrix and multiparameter estimation, J. Phys. A: Math. Theor. **53**, 023001 (2020).

[58] J. Liu, M. Zhang, H. Chen, L. Wang, and H. Yuan, Optimal scheme for quantum metrology, Adv. Quantum Technol. **5**, 2100080 (2022).

[59] P. Kok and S. L. Braunstein, Detection devices in entanglement-based optical state preparation, Phys. Rev. A **63**, 033812 (2001).

[60] R. H. Hadfield, G. Johansson, *et al.*, *Superconducting devices in quantum optics* (Springer, 2016).

[61] K. Banaszek and I. A. Walmsley, Photon counting with a loop detector, Opt. Lett. **28**, 52 (2003).

[62] G. S. Agarwal, *Quantum optics* (Cambridge University Press, 2012).

[63] P. A. Whitlock and M. H. Kalos, *Monte Carlo Methods* (New York: Wiley, 1986).

[64] L. Tierney, Markov chains for exploring posterior distributions, The Annals of Statistics **22**, 1701 (1994).

[65] W. K. Hastings, Monte carlo sampling methods using markov chains and their applications, Biometrika **57**, 97 (1970).

AUTHOR CONTRIBUTIONS

H.D. and Z.C.Z. conceived the idea and Z.C.Z. performed the calculations. H.D. and Z.C.Z. wrote the manuscript. X.Z. and J.L. contributed to the discussion and reviewed the manuscript.

COMPETING INTERESTS

The authors declare no competing interests.